optica

Quantum-enhanced interferometry with weak thermal light: supplementary material

SEYED MOHAMMAD HASHEMI RAFSANJANI[1,*], MOHAMMAD MIRHOSSEINI[1], OMAR S. MAGAÑA-LOAIZA[1], BRYAN T. GARD[2], RICHARD BIRRITTELLA[3], B. E. KOLTENBAH[4], C. G. PARAZZOLI[4], BARBARA A. CAPRON[4], CHRISTOPHER C. GERRY[3], JONATHAN P. DOWLING[2], AND ROBERT W. BOYD[1,5]

[1] *Institute of Optics, University of Rochester, Rochester, New York 14627*
[2] *Hearne Institute for Theoretical Physics and Department of Physics and Astronomy, Louisiana State University, Baton Rouge, LA 70803*
[3] *Department of Physics and Astronomy, Lehman College, The City University of New York, Bronx, New York 10468*
[4] *Boeing Research & Technology, Seattle, WA 98124*
[5] *Department of Physics, University of Ottawa, Ottawa, ON, K1N6N5, Canada*
[*] *Corresponding author: shashem2@ur.rochester.edu*

Published 20 April 2017

This document provides supplementary information to "Quantum-enhanced interferometry with weak thermal light," https://doi.org/10.1364/optica.4.000487. The mathematical model behind photon subtraction, a discussion on the photon distribution, an explanation about common-path interferometers, and information on the photon counting scheme are presented below.

https://doi.org/10.1364/optica.4.000487.s001

1. PHOTON SUBTRACTION

In the following we present a detailed calculation of the effect of the subtraction on the quantum state of a photon that leaves a Mach-Zehnder interferometer. The two input ports of the interferometer (a, b) are fed by a thermal state and the vacuum state respectively (See Fig. S1). Let us first derive the the reduced density matrix at the two output ports (c, d). A schematic version of the model is given in Fig. S1 The output ports are related to the input ports through a unitary transformation:

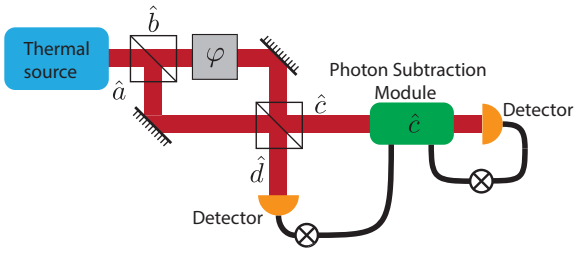

Fig. S1. Conceptual representation of a thermal interferometry experiment to observe the enhancement of signal and signal-to-noise ratio as result of photon subtraction.

$$\hat{c} = \frac{1}{2}\left\{iy\hat{a} - x\hat{b}\right\}$$
$$\hat{d} = \frac{1}{2}\left\{iy\hat{b} + x\hat{a}\right\} \quad \textbf{(S1)}$$

where $x = 1 - e^{i\varphi}$, and $y = e^{i\varphi} + 1$. The input state is given by

$$\hat{\rho}_0 = \sum_n \frac{\bar{n}^n}{(1+\bar{n})^{n+1}} |n\rangle_a \, {}_a\langle n| \otimes |0\rangle_b \, {}_b\langle 0|. \quad \textbf{(S2)}$$

The reduced density matrix of the state at port c can be derived by taking a partial trace on d:

$$\hat{\rho}_{0c} = \mathrm{Tr}_d[\hat{\rho}_0] = \sum_{m=0}^{\infty} {}_d\langle m|\hat{\rho}_0|m\rangle_d \quad \textbf{(S3)}$$

To evaluate this density matrix we need to calculate the following quantity

$$\begin{aligned}\mathcal{A}_{m,n} &= {}_d\langle m| \otimes {}_c\langle n|\hat{\rho}_0|n\rangle_c \otimes |m\rangle_d \\ &= \frac{1}{m!n!} {}_d\langle 0| \otimes {}_c\langle 0|d^m c^n \hat{\rho}_0 c^{\dagger n} d^{\dagger m}|0\rangle_c \otimes |0\rangle_d \end{aligned} \quad \textbf{(S4)}$$

Note that $|0\rangle_c \otimes |0\rangle_d = |0\rangle_a \otimes |0\rangle_b$, and we can expand this expression to evaluate it;

$$\begin{aligned}\mathcal{A}_{m,n} &= \frac{1}{m!n!4^{m+n}}\, {}_a\langle 0| \otimes {}_b\langle 0|(-x\hat{b}+iy\hat{a})^n \\ &\quad (iy\hat{b}+x\hat{a})^m \hat{\rho}_{th}^{(a)} \otimes |0\rangle_b\, {}_b\langle 0|(-iy\hat{b}^\dagger + x\hat{a}^\dagger)^m \\ &\quad (-x\hat{b}^\dagger - iy\hat{a}^\dagger)^n |0\rangle_a \otimes |0\rangle_b \\ &= \frac{|x|^{2m}|y|^{2n}}{m!n!4^{m+n}}\, {}_a\langle 0|\hat{a}^{n+m}\hat{\rho}_{th}^{(a)}\hat{a}^{\dagger(n+m)}|0\rangle_a \\ &= \frac{|x|^{2m}|y|^{2n}}{m!n!4^{m+n}} \sum_i \frac{\bar{n}^i |\,{}_a\langle 0|\hat{a}^{n+m}|i\rangle_a|^2}{(1+\bar{n})^{i+1}} \\ &= \frac{|x|^{2m}|y|^{2n}(m+n)!}{m!n!4^{m+n}} \frac{\bar{n}^{m+n}}{(1+\bar{n})^{m+n+1}} \end{aligned} \quad \textbf{(S5)}$$

Using this result one can calculate the diagonal elements of the reduced density matrix.

$$\begin{aligned}{}_c\langle n|\hat{\rho}_c|n\rangle_c &= \sum_m \mathcal{A}_{m,n} \\ &= \frac{|y|^{2n}\bar{n}^n}{4^n(1+\bar{n})^{n+1}} \sum_m \binom{n+m}{m} \left(\frac{\bar{n}|x|^2}{4(1+\bar{n})}\right)^m \\ &= \frac{|y|^{2n}\bar{n}^n}{4^n(1+\bar{n})^{1+n}} \left(\frac{1}{1-\frac{\bar{n}|x|^2}{4(1+\bar{n})}}\right)^{n+1} \\ &= \frac{|y|^{2n}\bar{n}^n}{4^n} \frac{1}{(1+\frac{\bar{n}|y|^2}{4})^{n+1}} \end{aligned} \quad \textbf{(S6)}$$

Furthermore one can readily confirm that $\langle i|\hat{\rho}_c|j\rangle$ vanishes if $i \neq j$. Thus the density matrix at port $\hat{c}$ can be written as

$$\hat{\rho}_c = \sum_n \frac{(\bar{n}\cos^2\frac{\varphi}{2})^n}{(1+\bar{n}\cos^2\frac{\varphi}{2})^{n+1}} |n\rangle_c\, {}_c\langle n| \quad \textbf{(S7)}$$

which a thermal state with the reduced occupation number and standard deviation of

$$\bar{n}_c = \mathrm{Tr}[\hat{c}^\dagger\hat{c}\hat{\rho}_c] = \bar{n}\cos^2\frac{\varphi}{2}, \qquad \sigma_c = \sqrt{\bar{n}_c^2 + \bar{n}_c} \quad \textbf{(S8)}$$

Similarly one can show that the reduced density matrix at port $\hat{d}$ is a thermal state with the reduced occupation number and standard deviation of

$$\bar{n}_d = \mathrm{Tr}[\hat{d}^\dagger\hat{d}\hat{\rho}_0] = \bar{n}\sin^2\frac{\varphi}{2}, \qquad \sigma_d = \sqrt{\bar{n}_d^2 + \bar{n}_d} \quad \textbf{(S9)}$$

Next we study the effect of photon subtraction on the reduced density matrices at output ports. Subtracting a photon in port $\hat{c}$ can be described by the following operation:

$$\hat{\rho}_0 \to \hat{\rho}_1 = \frac{\hat{c}\hat{\rho}_0\hat{c}^\dagger}{\mathrm{Tr}[\hat{c}\hat{\rho}_0\hat{c}^\dagger]}. \quad \textbf{(S10)}$$

By taking partial trace one can then find the reduced density matrix at each of the output ports.

$$\hat{\rho}_{1c} = \mathrm{Tr}_d[\hat{\rho}_1].$$

First we note that

$${}_d\langle m| \otimes {}_c\langle n|\hat{\rho}_1|n\rangle_c \otimes |m\rangle_d = \frac{n+1}{\bar{n}_c}\mathcal{A}_{m,n+1} \quad \textbf{(S11)}$$

Thus the diagonal elements of the reduced density matrix can be found as following

$${}_c\langle n|\hat{\rho}_c|n\rangle_c = \frac{n+1}{\bar{n}_c}\sum_m \mathcal{A}_{m,n+1} = \frac{(n+1)\bar{n}_c^n}{(1+\bar{n}_c)^{n+2}} \quad \textbf{(S12)}$$

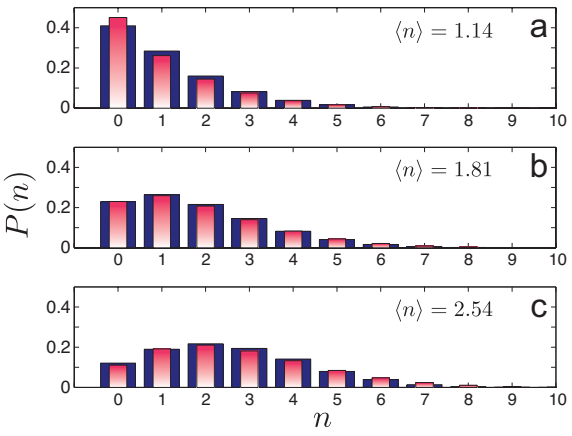

Fig. S2. (a) Photon distribution for the thermal light distribution that we used in the experiment. (b) Photon number distribution for the photon-subtracted thermal light. (c) Photon number distribution for the two-photon-subtracted thermal light. The dark bars represent the experimental results and the bright bars are the corresponding theory predictions.

One can readily confirm that the off-diagonal elements are all zero and thus the reduced density matrix in port $\hat{c}$ after the subtraction are given by

$$\hat{\rho}_{1c} = \sum_n \frac{(n+1)\bar{n}_c^n}{(1+\bar{n}_c)^{n+2}} |n\rangle_c\, {}_c\langle n|. \quad \textbf{(S13)}$$

The average occupation number and the standard deviation of this distribution are

$$\begin{aligned}\mathrm{Tr}[\hat{c}^\dagger\hat{c}\hat{\rho}_1] &= 2\bar{n}\cos^2\frac{\varphi}{2} = 2\bar{n}_c \\ (\mathrm{Tr}[(\hat{c}^\dagger\hat{c})^2\hat{\rho}_1] - \mathrm{Tr}[\hat{c}^\dagger\hat{c}\hat{\rho}_1]^2)^{1/2} &= \sqrt{2}\sigma_c \end{aligned} \quad \textbf{(S14)}$$

Note that the standard deviation increases only by a factor of $\sqrt{2}$ whereas the signal is multiplied by a factor of 2, and thus the signal-to-noise ratio is enhanced by a factor of $\sqrt{2}$. Similarly one can show that the conditioned on subtracted events in mode $\hat{c}$ the average occupation number in port $\hat{d}$ doubles and the standard deviation is enhanced by a factor of $\sqrt{2}$ too.

$$\begin{aligned}\mathrm{Tr}[\hat{d}^\dagger\hat{d}\hat{\rho}_1] &= 2\bar{n}\sin^2\frac{\varphi}{2} = 2\bar{n}_d \\ (\mathrm{Tr}[(\hat{d}^\dagger\hat{d})^2\hat{\rho}_1] - \mathrm{Tr}[\hat{d}^\dagger\hat{d}\hat{\rho}_1]^2)^{1/2} &= \sqrt{2}\sigma_d \end{aligned} \quad \textbf{(S15)}$$

We emphasize that this surprising result could be expected since, in contrast with the input ports, the density matrix at the output ports are correlated.

2. PHOTON DISTRIBUTION

When a beam of light that can be described by a coherent state is passed through a rotating ground glass light is scattered in a speckle pattern. If light from this scattering is coupled into a single-mode fiber the emerging light possess thermal distribution. In Fig. (S2 a) we plot this distribution and compare it with the theory. For the sake of completeness we have also included plots for the one-photon subtracted state and two-photon subtracted states in Fig. (S2 b) and Fig. (S2 c)

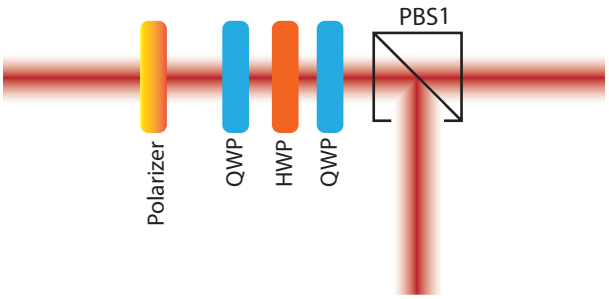

Fig. S3. A schematic representation of a common-path Mach-Zehnder interferometer that induces a variable phase between the two polarizations.

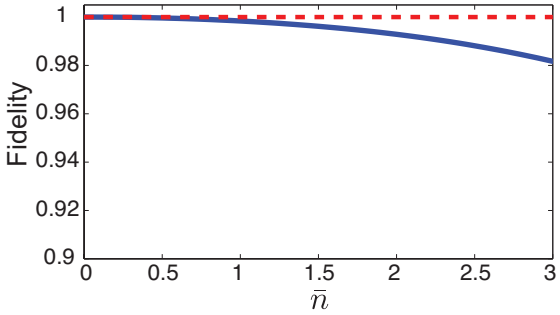

Fig. S4. The fidelity between the probability distribution of thermal statistics and the probability distribution detected by our photon counting scheme for thermal lights of different values of average occupation number.

3. COMMON PATH MACH-ZEHNDER INTERFEROMETER

In a conventional Mach-Zehnder interferometer the first beam splitter separates the beam into two parts. Each part takes a separate path and and then we bring the two paths together and recombine them using another beam splitter. The difference between the accumulated phase of the paths determines the intensity distribution at the two output ports. A challenging aspect of an MZI is its stability; A slight instability in any of the components would lead to phase instability and diminishes the fringe visibility. To alleviate this problem one can replace the two spatially separated paths by polarization, and uses wave plates to induce a phase between the two polarizations. As such one no longer needs to separate the two polarizations spatially, and can considerably mitigate the instability of the system.

Below we present a detailed discussion on how this interferometer works. In Fig. S3 we present a schematic representation of a common-path Mach-Zehnder interferometer. The polarizer prepares the polarization state $|H\rangle$ which can be written as an equally wighted coherent superposition of $|D\rangle$ and $|A\rangle$. Note that here

$$|D\rangle = \frac{|H\rangle + |V\rangle}{\sqrt{2}},$$
$$|A\rangle = \frac{|H\rangle - |V\rangle}{\sqrt{2}}. \quad \textbf{(S16)}$$

Our aim is to induce a phase between the two components $|D\rangle$ and $|A\rangle$. Then we set a quarter wave-plate (QWP) in a 45° angle. The QWP maps $|D\rangle \rightarrow |R\rangle$, and $|A\rangle \rightarrow |L\rangle$ where

$$|R\rangle = \frac{|H\rangle + i|V\rangle}{\sqrt{2}},$$
$$|L\rangle = \frac{|H\rangle - i|V\rangle}{\sqrt{2}}. \quad \textbf{(S17)}$$

Next we can use a half wave-plate that induces a variable phase between the two components $|R\rangle$ and $|L\rangle$. Again a QWP can be used to map $|R\rangle \rightarrow |D\rangle$ and $|L\rangle \rightarrow |A\rangle$, and finally we use a polarizing beam splitter to separate the two polarizations $|D\rangle$ and $|A\rangle$. By rotating the HWP we can change the induced phase between the two polarizations $|D\rangle$ and $|A\rangle$ and we get a one-to-one mapping between this setup and a conventional Mach-Zehnder interferometer.

4. SURJECTIVE PHOTON COUNTING

We emphasize that the effect of the inherent quantum efficiency of the detector can be modeled by combination of a beam splitter and a detector of quantum efficiency of 100%. That is a detector that fires if at least one photon arrives. Thus for simplifying our analysis we assume a detector with detection efficiency of 100%. For thermal light with average occupation number of $\bar{n}$ the probability of incurring an N-photon event is given by

$$P(N) = \frac{\bar{n}^N}{(1+\bar{n})^{N+1}}. \quad \textbf{(S18)}$$

In our surjective detection scheme this event may be registered as a detection of a lower number of photons if more than one photons arrive separated by less than the dead time of the detector. Assuming that the dead time of the detector time is $\sim 50\,ns$ and the coherence time of the source is $\sim\ 1\mu s$ in each coherence time there are $K = 20$ time bins. In principle an N-photon event can be registered as any of $\{1, 2, \cdots, N\}$-photon events, and since we work with very few photons we assume that always $K > N$. Then the probability distribution of number of clicks if N photons arrive in a temporal mode can be cast as a combinatorics problem and one uses Bayes' theorem:

$$P(m) = \sum_N P(N)P(m|N). \quad \textbf{(S19)}$$

to find the modified probability distribution, $P(m)$, that the APDs register. In Fig. S4 we plot the fidelity between the probability distribution of the thermal statistics and the probability distribution detected by the our surjective counting scheme. Fidelity is a measure of distance between any two probability distributions. The fidelity of two probability distributions $\{q_i\}$ and $\{p_i\}$ is defined by $\sum_i \sqrt{p_i q_i}$ and its range between $\{0, 1\}$ [1]. The high value of the fidelity confirms our initial intuition that for low photon number, our counting scheme provides an excellent approximation to the actual photon distribution. Finally it should be noted that to compare with the experimental results one can feed the probability distributions that are predicted by the theory into an algorithm that counts for the surjective nature of the counting mechanism before comparing them to the experimental results.

REFERENCES

1. M. A. Nielsen and I. L. Chuang, *Quantum Computation and Quantum Information*, 10th Anniversary Edition (Cambridge University Press, Cambridge, 2009).